

Electronic Supplementary Information

B₃@Si₁₂⁺: Strong stabilizing effects of triatomic cyclic boron unit on tubular silicon clusters

Hung Tan Pham,^{a,b} Dang Thi Tuyet Mai,^d Long Van Duong,^c

Nguyen Minh Tam^{a,b} and Minh Tho Nguyen^{a,b,d,*}

^a Computational Chemistry Research Group, Ton Duc Thang University, Ho Chi Minh City, Vietnam

^b Faculty of Applied Sciences, Ton Duc Thang University, Ho Chi Minh City, Vietnam

^c Institute for Computational Science and Technology at Ho Chi Minh City (ICST)

^d Department of Chemistry, KU Leuven, Celestijnenlaan 200F, B-3001 Leuven, Belgium

Emails: nguyenminhtho@tdt.edu.vn; minh.nguyen@kuleuven.be

Table of content:

Figure S1. Shapes, symmetries and relative energies (ΔE , kcal/mol) of lower-lying structures of BSi₁₂⁺ using DFT and G4 methods. Values given in square brackets, brackets and curly brackets are from TPSSh, B3LYP, PBE0PBE/6-311+G(d) computations with ZPE corrections.

Figure S2. Shapes, symmetries and relative energies (ΔE , kcal/mol) of the lower-lying structures of B₂Si₁₂ neutral using DFT and G4 methods. Values given in square brackets, brackets and curly brackets are from TPSSh, B3LYP, PBE0PBE/6-311+G(d) computations with ZPE corrections.

Figure S3. Shapes, symmetries and relative energies (ΔE , kcal/mol) of the lower-lying structures of B₃Si₁₂ cation using DFT and G4 methods. Values given in square brackets, brackets and curly brackets are from TPSSh, B3LYP, PBE0PBE/6-311+G(d) computations with ZPE corrections.

Figure S4. The root mean squared deviation in molecular dynamics (MD) simulations of B₃Si₁₂⁺.

Figure S5. The Laplacian iso-surface with bon critical point (BCP, green ball) and ring critical point (RCP, red ball) of B₂Si₁₂ and B₃Si₁₂⁺.

Figure S6. Magnetic ring current maps of B₂Si₁₂ and B₃Si₁₂⁺.

Figure S7. The line stream of current density provided by GIMIC calculations for Si₁₂ and B₃^{+/−} clusters.

Table: Cartesian Coordinates of the main structures considered.

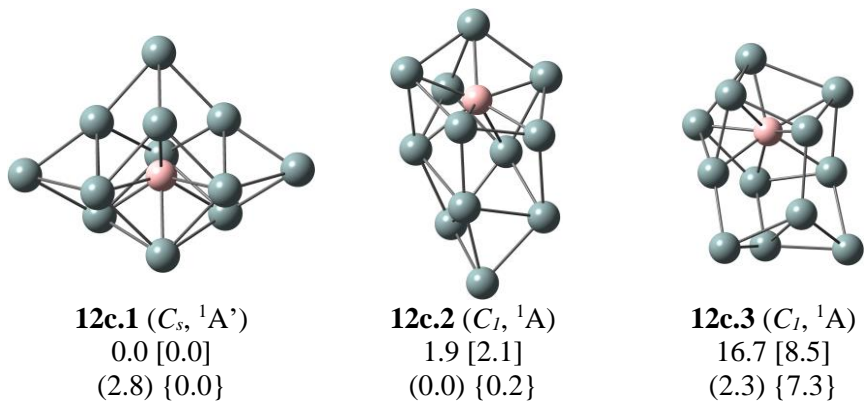


Figure S1.

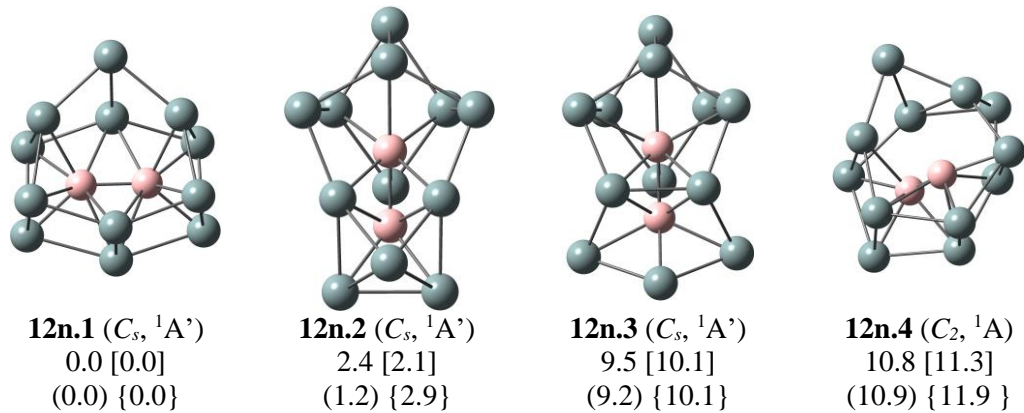


Figure S2.

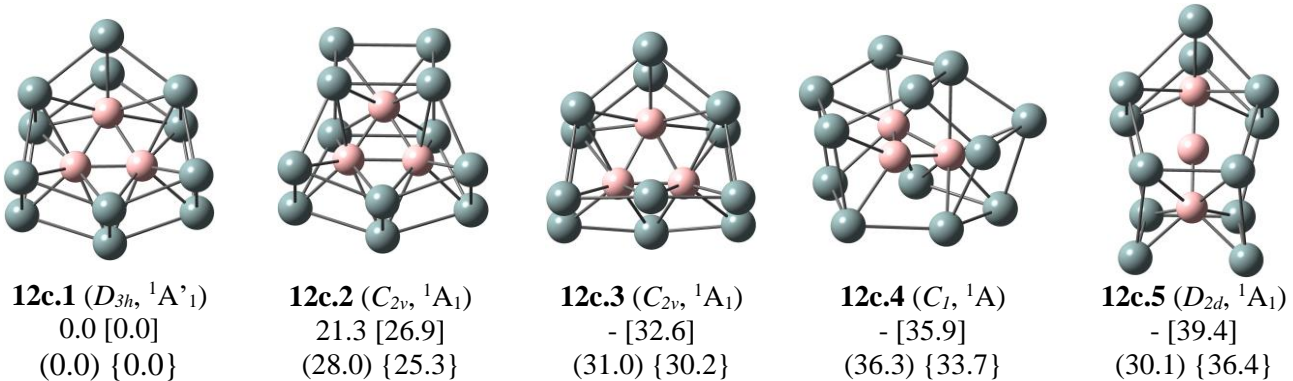


Figure S3.

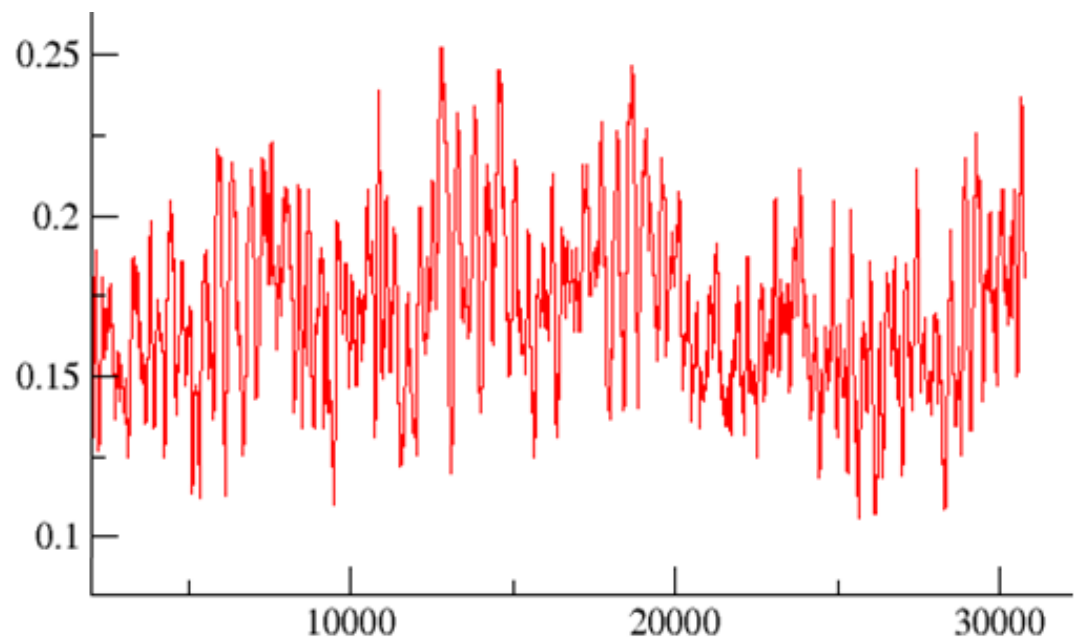


Figure S4.

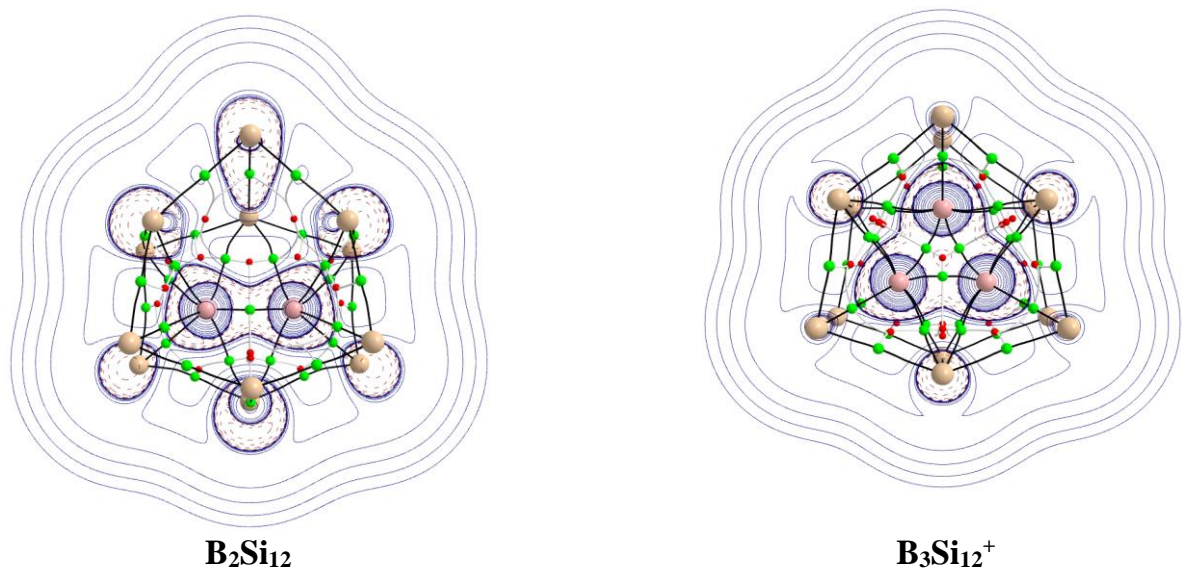
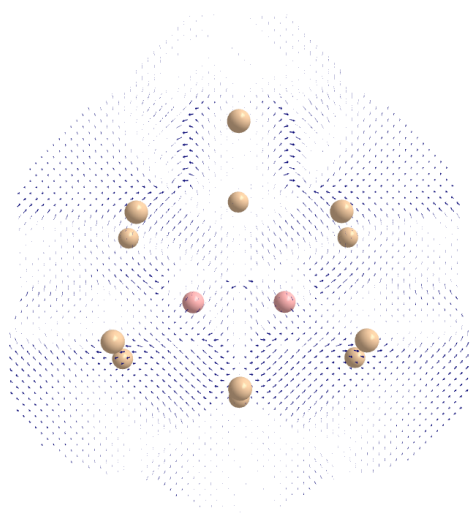
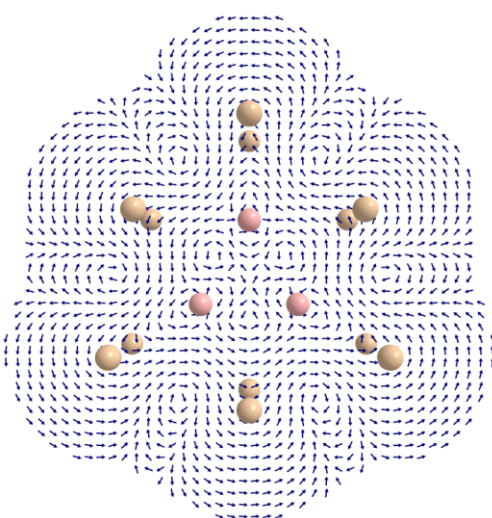


Figure S5.

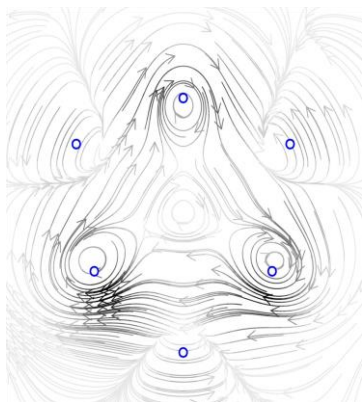


B_2Si_{12}

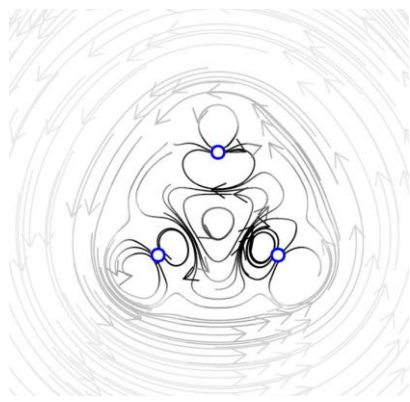


$\text{B}_3\text{Si}_{12}^+$

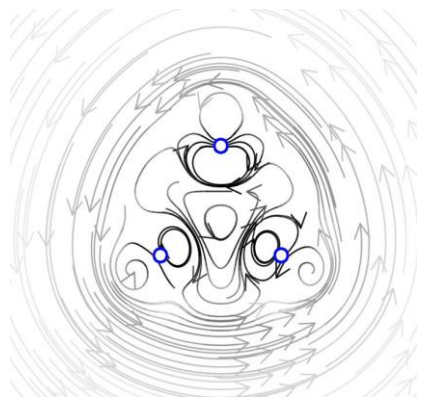
Figure S6.



Si_{12}



B_3^+



B_3^-

Figure S7.

Table: Cartesian coordinates of **3.cA**, **2.n.A** and **1.c.A**

3.c.A

B	0.00000000	-1.00494006	0.00000000
B	0.87030362	0.50247003	0.00000000
B	-0.87030362	0.50247003	0.00000000
Si	0.00000000	2.20478101	1.18333109
Si	2.29172883	1.32313025	1.30965506
Si	1.90939637	-1.10239051	1.18333109
Si	-0.00000000	-2.64626051	-1.30965506
Si	-0.00000000	-2.64626051	1.30965506
Si	-2.29172883	1.32313025	1.30965506
Si	-1.90939637	-1.10239051	-1.18333109
Si	-2.29172883	1.32313025	-1.30965506
Si	-0.00000000	2.20478101	-1.18333109
Si	1.90939637	-1.10239051	-1.18333109
Si	2.29172883	1.32313025	-1.30965506
Si	-1.90939637	-1.10239051	1.18333109

2.n.A

Si	-1.48281604	0.86365693	-2.26025190
Si	-1.13899367	1.59294541	0.00000000
Si	-1.48281604	0.86365693	2.26025190
Si	-0.98685470	-1.56123830	2.35442720
Si	-0.72896363	-2.31277486	0.00000000
Si	-0.98685470	-1.56123830	-2.35442720
Si	1.45932666	-0.86854169	2.22614710
Si	1.55383787	-1.69446015	0.00000000
Si	1.45932666	-0.86854169	-2.22614710
Si	0.82328736	1.39062725	1.85031800
Si	0.82328736	1.39062725	-1.85031800
Si	0.81228090	3.00892043	0.00000000
B	-0.17366723	-0.34109487	-0.88098190
B	-0.17366723	-0.34109487	0.88098190

1.c.A

B	-0.25473299	-0.00013102	0.00000000
Si	-2.35751886	0.46565460	0.00000000
Si	-0.72032657	1.44354011	1.67576300
Si	1.18291391	-0.32360645	-1.68554400
Si	0.36025537	-2.14335020	0.00000000
Si	-0.17844399	0.00042195	3.59052900
Si	1.18291391	-0.32360645	1.68554400
Si	-1.23308334	-1.16338073	-1.65529300

Si	2.94132901	0.00181103	0.00000000
Si	1.04479053	1.76198159	0.00000000
Si	-0.17844399	0.00042195	-3.59052900
Si	-0.72032657	1.44354011	-1.67576300
Si	-1.23308334	-1.16338073	1.65529300